Wang et al. *Zool. Res.* 2024, 45(5): 961−971
https://doi.org/10.24272/j.issn.2095-8137.2024.030
https://cstr.cn/32248.14.zr.2024.030

ZR | Zoological Research

Article Open Access

Myotis bat STING attenuates aging-related inflammation in female mice

Xi Wang[1,2,3,#], Jing-Kun Jia[1,2,3,#], Qi Wang[1,2,3,#], Jing-Wen Gong[1], Ang Li[2,4], Jia Su[1,2,3], Peng Zhou[1,2,4,*]

[1] *Wuhan Institute of Virology*, *Chinese Academy of Sciences*, *Wuhan*, *Hubei* 430071, *China*

[2] *Guangzhou National Laboratory*, *Guangzhou International Bio Island*, *Guangzhou*, *Guangdong* 510005, *China*

[3] *University of Chinese Academy of Sciences*, *Beijing* 100000, *China*

[4] *State Key Laboratory of Respiratory Disease*, *First Affiliated Hospital of Guangzhou Medical School*, *Guangzhou*, *Guangdong* 510005, *China*

ABSTRACT

Bats, notable as the only flying mammals, serve as natural reservoir hosts for various highly pathogenic viruses in humans (e.g., SARS-CoV and Ebola virus). Furthermore, bats exhibit an unparalleled longevity among mammals relative to their size, particularly the *Myotis* bats, which can live up to 40 years. However, the mechanisms underlying these distinctive traits remain incompletely understood. In our prior research, we demonstrated that bats exhibit dampened STING-interferon activation, potentially conferring upon them the capacity to mitigate virus- or aging-induced inflammation. To substantiate this hypothesis, we established the first *in vivo* bat-mouse model for aging studies by integrating *Myotis davidii* bat STING (*Md*STING) into the mouse genome. We monitored the genotypes of these mice and performed a longitudinal comparative transcriptomic analysis on *Md*STING and wild-type mice over a 3-year aging process. Blood transcriptomic analysis indicated a reduction in aging-related inflammation in female *Md*STING mice, as evidenced by significantly lower levels of pro-inflammatory cytokines and chemokines, immunopathology, and neutrophil recruitment in aged female *Md*STING mice compared to aged wild-type mice *in vivo*. These results indicated that *Md*STING knock-in attenuates the aging-related inflammatory response and may also improve the healthspan in mice in a sex-dependent manner. Although the underlying mechanism awaits further study, this research has critical implications for bat longevity research, potentially contributing to our comprehension of healthy aging in humans.

Keywords: Bat; STING; Longevity; Aging-related inflammation; Virus reservoir host

INTRODUCTION

As the only mammals capable of powered flight, bats exhibit a multitude of distinctive biological traits (Déjosez et al., 2023; Irving et al., 2021; Teeling et al., 2018). Bats are also recognized as natural reservoir hosts for diverse highly pathogenic viruses, some of which have precipitated large-scale infectious diseases in humans, such as SARS-related coronaviruses and Ebola virus (Déjosez et al., 2023; Irving et al., 2021; Ruiz-Aravena et al., 2022; Teeling et al., 2018). Bats are also noted for their unparalleled longevity among mammals relative to their size (Austad, 2009; Brunet-Rossinni & Austad, 2004; Power et al., 2022), with those within the genus *Myotis* exhibiting the greatest longevity, living up to 40 years (Healy et al., 2014). However, the mechanisms underlying these unique characteristics, particularly their roles as viral reservoir hosts and long-lived animals, remain inadequately understood.

In recent years, research efforts have predominantly centered on unraveling the coexistence of bats and viruses (Déjosez et al., 2023; Irving et al., 2021; Ruiz-Aravena et al., 2022; Teeling et al., 2018). Our work, along with that of other researchers, has revealed that bats maintain a constitutively expressed interferon system, with a simultaneous dampening of stimulator of interferon gene (STING) expression and inflammatory response (Ahn et al., 2019; Fu et al., 2023; Xie et al., 2018; Zhou et al., 2016). These characteristics may enable early inhibition of viral replication or moderate the immune response upon viral infection. Notably, a low-level, overactive inflammatory response is also a hallmark of human aging, attributed to the senescence-associated secretory phenotype (SASP), which largely depends on the DNA-cGAS-STING pathway (Gulen et al., 2023; Pan et al., 2023; Victorelli et al., 2023; Zhang et al., 2022; Zhao et al., 2023). Therefore, it is conceivable that the dampened STING/NLRP3

Received: 29 January 2024; Accepted: 12 April 2024; Online: 13 April 2024
Foundation items: This work was supported by the China Natural Science Foundation for Outstanding Scholars (82325032) and Self-Supporting Program of Guangzhou Laboratory (SRPG22-001)

[#]Authors contributed equally to this work

*Corresponding author, E-mail: zhou_peng@gzlab.ac.cn

inflammatory responses observed in bats may contribute to the mitigation of aging-related inflammation, potentially extending their healthspan (Ahn et al., 2019; Xie et al., 2018). Longitudinal comparative transcriptomic analysis has shown that bats display a unique, age-related gene expression pattern associated with DNA repair, autophagy, immunity, and tumor suppression, suggesting these factors may be instrumental in driving their prolonged healthspan (Huang et al., 2019). However, it is important to note that these observations are primarily observational and lack *in vivo* confirmation. Remarkably, until the bat ASC2-mouse study conducted last year, *in vivo* research into bat functional genes has been scarce due to existing limitations in gene modulation in these species (Ahn et al., 2023). A recent study demonstrated prolonged healthspan in a transgenic mouse overexpressing naked mole-rat hyaluronic acid synthase 2 gene (Zhang et al., 2023), providing a valuable paradigm for characterizing unique genes associated with lifespan and healthspan in model organisms.

We previously identified a universal replacement of the serine 358 residue (a critical activation residue) in STING in bats, leading to attenuated downstream interferon responses and antiviral activity (Xie et al., 2018). In recent years, extensive research has explored the role of STING in the human aging process (Huang et al., 2023; Pan et al., 2023; Paul et al., 2021). Studies have shown that the cGAS-STING pathway acts as a driver of the senescence-associated secretory phenotype (SASP) in humans, and inhibiting cGAS-STING signaling may be a potential strategy for impeding neurodegenerative processes in old age (Gulen et al., 2023; Zhang et al., 2022; Zhao et al., 2023). Consequently, we hypothesized that the uniquely dampened character of STING in bats may contribute to their relatively extended healthspan. In this study, we established a *Myotis davidii* bat STING (*Md*STING)-knock-in mouse model and conducted a comprehensive comparative analysis of aging-related genotypes with wild-type (WT) mice over a 3-year period. To the best of our knowledge, this represents the first animal model in the field of bat aging, paving the way for unraveling the mechanisms underpinning the exceptional longevity observed in bats.

MATERIALS AND METHODS

Establishment of *Myotis* STING mouse model

C57BL/6J WT mice were purchased from Beijing Vital River Laboratory Animal Technology Co., Ltd. (China). The design, establishment, and validation of *Md*STING mice were conducted by the authors and Shanghai Biomodel Organism Science & Technology Development Co., Ltd. (China) (Figure 1; Supplementary Figure S1). Briefly, the *MdSTING*$^{+/+}$ (*Md*STING) mice utilized in this study were generated through micro-injection of a donor vector, *in vivo*-transcribed Cas9 mRNA, and gRNA (GTGACCTCTGGGCCGTGGGA) into fertilized ovum (C57BL/6J background). The donor vector contained 5'/3' homologous arms and *MdSTING*-WPRE-poly A sequences. The *MdSTING*-WPRE-poly A sequences were precisely inserted downstream of the ATG start codon in the third exon of the mouse *Sting* gene, guaranteeing accurate transcriptional expression of the bat *STING* gene. Simultaneously, the mouse *Sting* gene was disrupted through targeted knockout during the knock-in procedure.

All animal experiments conducted in this study received approval from the Ethics Committee of the Wuhan Institute of Virology, Chinese Academy of Sciences, under approval number WIVA43202105. The experiments were conducted according to the fundamental guidelines for the welfare of experimental animals.

Cell culture and transfection

293T cells were cultured in Dulbecco's Modified Eagle Medium (DMEM) (Gibco, USA) supplemented with 10% (v/v) fetal bovine serum (FBS) (Gibco, USA) under 5% CO_2 at 37°C. *Myotis davidii*, *Homo sapiens*, and *Mus musculus STING* genes were cloned into the pCAGGS vector with a C-terminal S-tag. Before transfection, the correctness of STING plasmids was confirmed by sequencing. Transfections were conducted using Lipofectamine 3000 reagent (Thermo Scientific, USA) according to the manufacturer's protocols. Primary mouse bone marrow cells were harvested and differentiated into bone marrow-derived macrophages (BMDMs) over 6 days using RPMI 1640 supplemented with 10% (v/v) FBS and 20 ng/mL macrophage colony-stimulating factor (M-CSF) (PeproTech, USA) under 5% CO_2 at 37°C. Splenocytes were obtained by pressing spleen tissues through a cell strainer using a disposable abrasive stick. The collected splenocytes were then treated with 1×red blood cell (RBC) lysis buffer (eBioscience, USA). Subsequently, the splenocytes were washed twice with phosphate-buffered saline (PBS) and resuspended in RPMI 1640 supplemented with 10% (v/v) FBS.

Mouse genotype determination

Genotype determination of mice was performed at 2 weeks of age. Toes were excised and lysed in 300 μL of 50 mmol/L NaOH at 95°C for 30 min. Subsequently, 25 μL of 1 mol/L Tris-HCl (pH 8.0) was added and thoroughly mixed. Following treatment, the lysed samples were utilized as templates for polymerase chain reaction (PCR)-based genotype determination. The following primers were used: Primer F :5'-GGGGCTCACATGTACACGCTCTG-3'; Primer R: 5'- CGCGCA CAGCCTTCCAGTAG-3'.

Lifespan study and sample collection

The WT/*MdSTING*$^{+/+}$ mice utilized in this study were segregated by sex and housed in the animal facility of the Wuhan Institute of Virology, Chinese Academy of Sciences. Each cage accommodated six mice, maintained under a 12-h light/dark cycle at a constant room temperature of 25°C. The lifespan of the WT/*MdSTING*$^{+/+}$ mouse cohorts (n=6 males or females for STING mice, n=5 males/9 females for WT mice) was monitored, starting from 3 months of age until death. Blood samples were also collected from each mouse using EDTA·2Na (BBI, China) as an anticoagulant at 3 (n=26), 6 (n=26), 9 (n=26), 12 (n=26), 15 (n=23), 18 (n=21), 24 (n=13), and 29 (n=3) months. Weight and mortality were recorded prior to each blood collection. Mice surviving until the 29th month were anesthetized and then euthanized. For pathological confirmation of the blood transcriptome data, female mice were selected at 1.5 and 13 months of age (n=4) and anesthetized with avertin, followed by blood sample collection from the eyeballs, and subsequent euthanasia. Tissue samples from the heart, liver, spleen, lung, kidney, intestine, brain, and muscle were collected and partitioned into multiple portions for further analysis. Tissues intended for reverse transcription-quantitative real-time polymerase chain reaction (RT-qPCR) were directly preserved in tubes

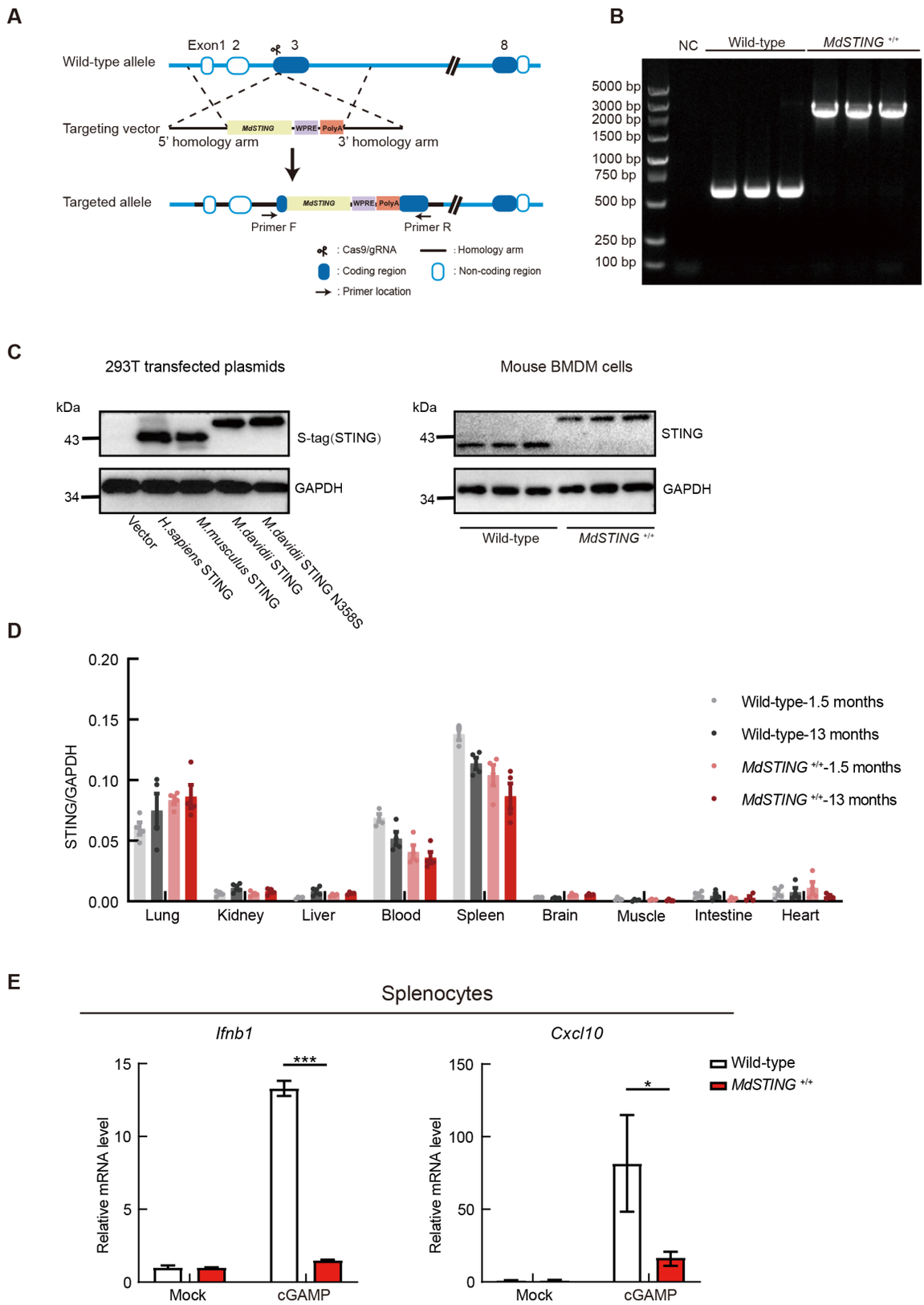

Figure 1 Validation of successful establishment of bat STING knock-in mice

A: Schematic of bat STING knock-in mouse generation. Primers (F and R) used for genotype identification were designed. B: Representative images of agarose gel electrophoresis for *Md*STING mice genotyping. C: Western blot analysis of STING protein to detect exogenous transfected STING plasmids in 293T cells (left) or endogenous expression of STING in BMDM cells from WT (*n*=3) or *Md*STING mice (*n*=3) (right). D: mRNA expression of *STING* gene in different organs of mice (*n*=4 for each group). Primers used for *STING* gene were mouse- or bat-specific, as shown in Supplementary Table S1. E: Splenocytes of WT and *Md*STING mice (*n*=3, cells from three mice each group) were transfected with cGAMP (2 μg/mL), induction of *Ifnb* and *Cxcl10* genes was determined by RT-qPCR. Primers are listed in Supplementary Table S1. Data are mean±SEM. *P*-values were obtained using two-tailed unpaired *t*-test, ns: Not significant; *: $P<0.05$; **: $P<0.01$; ***: $P<0.001$; ****: $P<0.0001$.

containing VeZol Reagent (R411-02, Vazyme, China), along with beads for tissue homogenization. Tissues intended for hematoxylin and eosin (H&E) staining and immunohistochemical (IHC) analysis were fixed in 4% paraformaldehyde (PFA) (BL539A, Biosharp, China). Blood samples were fractionated for RNA extraction and enzyme-linked immunosorbent assay (ELISA) testing.

RNA extraction and RNA sequencing

Total RNA from blood samples was extracted using VeZol Reagent (R411-02, Vazyme, China) following the manufacturer's instructions. In brief, tissue samples in VeZol were initially homogenized using the Tissue Cell-destroyer 1000 (NZK, China) at recommended settings, followed by total RNA extraction as per the provided manual. RNA samples obtained from mouse blood were submitted to BGI (Beijing, China) for sequencing. RNA sequencing (RNA-seq) library construction and subsequent sequencing procedures were conducted at BGI. The filtered sequencing data were processed using a standard pipeline. In Linux, raw reads were aligned to the respective homologous genomes using HISAT2 (v.2.1.0) (Kim et al., 2019) and SAMtools (v.1.17) (Danecek et al., 2021). For data originating from WT mice, the mouse genome (GCF_000001635.27) (https://www.ncbi.nlm.nih.gov/datasets/genome/GCF_000001635.27/) was employed as a reference, while the edited genome was utilized for data derived from *Md*STING mice. Subsequently, StringTie (v.2.2.1) (Shumate et al., 2022) was employed for transcript assembly and qualification, using high-quality genome annotation. Only samples exhibiting an overall alignment rate exceeding 80% were selected for subsequent analyses. Genes consistently expressed across all samples were subjected to differential expression analysis using the R program (v.4.3.1) (https://www.r-project.org/). Samples were categorized based on age and sex. Transcriptomic alterations in gene expression were compared between *Md*STING and WT mice. DESeq2 (v.1.40.2) (Love et al., 2014) was used for differential gene expression analysis, with all parameters set to default. Raw read quality was assessed using FastQC (v.0.11.9) (https://www.bioinformatics.babraham.ac.uk/projects/fastqc/). The counts matrix was analyzed using R (v.4.2.1) (https://www.r-project.org/). The DESeq2 (v.1.36.0) package in R was employed for normalization and identification of differentially expressed genes (DEGs) (Love et al., 2014). Gene set enrichment analysis (GSEA) was conducted using the R package clusterProfiler (v.4.4.4) (Wu et al., 2021). The fractions of neutrophils and monocytes/macrophages were inferred using ImmuCellAI-mouse (v.0.1.0) (Miao et al., 2022). All statistical analyses were performed using Stats (v.4.2.1) (https://search.r-project.org/R/refmans/stats/html/00Index.html). Data visualization was achieved using pheatmap (v.1.0.12) (https://cran.r-project.org/web/packages/pheatmap/index.html) and ggplot2 (v.3.3.6) (Wickham, 2016).

Quantitative real-time PCR (qPCR)

The qPCR experiments were conducted using the CFX Duet Real-Time PCR system (Bio-Rad, USA). The PCR settings and mix preparation were based on the instructions provided by the HiScript II One Step RT-qPCR SYBR Green Kit (Q221, Vazyme, China). Specific primer pairs were employed to assess mRNA levels of the corresponding genes (Supplementary Table S1).

Western blot analysis

The 293T and BMDM cells were lysed using western and IP lysis buffer (Beyotime, China) supplemented with protease and phosphatase cocktail inhibitors (Thermo Fisher, USA) for 15 min. The lysates were then mixed with 6×sodium dodecyl sulfate (SDS) loading buffer and boiled at 95°C for 10 min. Equal amounts of protein were loaded onto gels for SDS-polyacrylamide gel electrophoresis (SDS-PAGE), then transferred onto 0.22 μm polyvinylidene fluoride (PVDF) membranes. The membranes were subsequently blocked with rapid blocking solution for 10 min, then incubated with primary antibodies (anti-S-tag, 1:3 000, Abcam, UK; anti-GAPDH, 1:5 000, Proteintech, China; anti-STING, 1:1 000, Cell Signaling Technology, USA) overnight at 4°C and washed with TBS containing 0.1% Tween for 30 min. The membranes were then incubated with secondary antibodies (horseradish peroxidase (HRP)-conjugated anti-mouse/rabbit IgG, 1:10 000, Proteintech, China) at room temperature for 1 h, followed by washing for another 30 min. Finally, the membranes were exposed to an ECL chemiluminescent substrate (Vazyme, China) using a ChemiDoc XRS$^+$ imaging system (Bio-Rad, USA).

ELISA

Plasma samples from female mice aged 1.5 and 13 months were collected (four mice per group). The plasma concentration of interleukin-1β (IL-1β) was quantified using a mouse IL-1β ELISA Kit (CME0015, 4ABio, China) according to the manufacturer's instructions.

H&E staining and IHC analysis

The livers of female mice aged 1.5 and 13 months were collected (n=4 in each group). Fresh tissues were fixed in 4% paraformaldehyde for 24 h, embedded in paraffin, and sectioned into 4-μm-thick slices for histological and IHC analyses. For histological assessment, the sections were stained with hematoxylin (Servicebio, China) to visualize the nuclei and then with eosin (Servicebio, China) to delineate the cytoplasm. This staining facilitated the observation of normal tissue morphology as well as the infiltration of immune cells. For IHC, sections were incubated with anti-mouse Ly6G primary antibody (GB11229, 1:300, rabbit, Servicebio, China), then stained with fluorescently labeled secondary antibodies (anti-rabbit FITC, GB22403, 1:200, Servicebio, China) and 4',6-diamidino-2-phenylindole (DAPI, G1012, Servicebio, China) for nuclear staining. Fiji ImageJ (NIH, USA) software was used for analysis of inflammatory cell area and positive cell counts in IHC staining.

Statistical analysis

Data are presented as mean±standard error of the mean (SEM), unless stated otherwise. The term 'n' denotes the number of animals per test group, with age and sex also noted. Randomly selected littermates were utilized for all experiments. Statistical analyses were conducted using GraphPad Prism v.8.4.3 (GraphPad, USA). P-values were derived from a two-tailed unpaired t-test. Lifespan data were analyzed using Kaplan-Meier survival curves, with P-values calculated using the log-rank test. All relevant P-values are depicted in the figures.

RESULTS

Establishment of *Myotis* bat STING knock-in mice

To elucidate the role of STING in the extended healthspan

observed in bats, we engineered knock-in mice harboring the *Myotis davidii STING* gene (*MdSTING*), which notably dampens interferon activation in response to viral or cGAMP stimulation (Xie et al., 2018). Employing CRISPR-Cas9 technology (Ma et al., 2018), we introduced the *Myotis davidii STING* gene into exon 3 of the mouse *Sting* gene in C57BL/6J WT mice (Figure 1A; Supplementary Figure S1). Homozygous *MdSTING*$^{+/+}$ mice were generated through heterozygous breeding, and the correct insertion of the *MdSTING* gene was confirmed via genomic DNA sequencing or PCR analysis (Figure 1B; Supplementary Figure S1A and Data S1). We also detected STING protein expression in the mice, which matched the size of the exogenously transfected STING protein (Figure 1C). Notably, the molecular weight of *Md*STING was naturally higher than that of human or mouse STING, likely due to differences in post-translational modifications such as glycosylation, as *Md*STING contains more O-glycosylation sites compared to that of mice and humans (Supplementary Figure S1B). The expression pattern of the *MdSTING* gene across various mouse organs was also verified, revealing no discernible differences compared to WT mice (Figure 1D). Furthermore, to validate the functionality of bat STING, we stimulated splenocytes from WT and bat STING knock-in mice with cGAMP. The data revealed that bat STING knock-in mice exhibited a dampened type I interferon response (Figure 1E), consistent with our previous study (Xie et al., 2018). Collectively, the *Myotis davidii STING* gene was successfully inserted into the mouse genome, demonstrating a correct size, similar expression pattern, and reduced interferon activation, comparable to the exogenously transfected *Myotis* STING protein in WT mice.

Longitudinal comparative transcriptomic analysis reveals reduced aging-related inflammation responses in bat STING knock-in mice

To explore whether *Md*STING attenuates aging-related inflammation and further improves the healthspan in mice, we conducted a longitudinal comparative study involving both WT and *Md*STING mice. The cohort, comprising an equal number of male and female mice, underwent continuous lifespan and body weight monitoring. Additionally, blood samples were collected from each mouse via retro-orbital bleeding at 0, 3, 6, 9, 12, 15, 18, 24, and 29 months of age for subsequent transcriptomic analysis (Figure 2A). The monitoring period spanned 37 months in total. Results revealed that both WT and bat STING knock-in mice maintained similar body weights throughout their lifespan (Supplementary Figure S2). Although not statistically significant, female *Md*STING mice demonstrated a trend toward extended median lifespan compared to control mice, a pattern not observed in male mice (Supplementary Figure S2). However, this observation of prolonged lifespan was based on a relatively small cohort size, and future studies are needed, including more animals of both sexes, for more robust conclusions.

Given the possible extended median lifespan observed in female *Md*STING mice, we further explored whether this gene contributed to an overall improvement in health status. Based on longitudinal comparative transcriptomic analysis of mouse blood during the aging process, we identified consistent patterns of gene regulation, both up-regulation and down-regulation, in aged mice (after 12 months) compared to their younger counterparts. Notably, female *Md*STING mice exhibited a marked alleviation in aging-related genes and pathways compared to WT female mice (Figure 2). These findings were not observed in male mice (Supplementary Figure S3). These results suggest that the introduction of *Md*STING may play a potential role in mitigating aging-related inflammation responses, contributing to the overall enhanced health status in these mice.

To determine the molecular pathways underlying the observed differences between aged *Md*STING and WT mice, we conducted GSEA on DEGs (Subramanian et al., 2005). Notably, pathways associated with neutrophil and TNF activation exhibited time-dependent lower expression in the aged *Md*STING mice (Figure 2B), indicating a potential role in STING-dependent aging-related inflammation (Victorelli et al., 2023). Additionally, enrichment of epidermal cell differentiation was also identified, likely due to regular retro-orbital bleeding damage. Further analysis revealed 4 864 pathways displaying consistent differences across all time points. Pathways linked to neutrophil activation, degranulation, and leukocyte inflammatory response were significantly down-regulated in aged *Md*STING mice compared to WT mice (Figure 2C, D). Conversely, pathways associated with the cell cycle were significantly up-regulated in aged *Md*STING mice (Figure 2E). Given that cell cycle arrest is a hallmark of aging (Cai et al., 2022), our findings suggest that the blood transcriptome of aged *Md*STING mice may exhibit characteristics akin to those of younger mice.

To further elucidate the implications of differential genes and pathways, we analyzed the inferred proportions of neutrophils, monocytes, and macrophages in both WT and *Md*STING mice at each time point (Figure 2F, G). Results indicated that *Md*STING mice exhibited lower overall levels of inflammatory myeloid cells, including neutrophils, monocytes, and macrophages, compared to WT mice (Figure 2F, G). Additionally, we examined the expression differences of a panel of inflammation-related genes in the blood transcripts between aged *Md*STING and WT mice. Notably, genes such as *Lcn2* (neutrophil cytokine signaling), *Ngp* (neutrophilic granule protein), *Cxcr2* (neutrophil, mononuclear macrophage chemokine receptor), *Ifngr1* (interferon gamma receptor), *Nlfam1* (monocyte pro-inflammatory responses), *Tnfaip3* (ameliorates degeneration of inflammatory response), *Il1b* (major inflammatory cytokine), *Il7r* (T cell activation-related receptor), and *Il17ra* (Il17 receptor, related to Th17 response) were significantly lower in aged *Md*STING female mice at various time points during the aging process (Supplementary Figure S4), but this pattern was not observed in aged male mice (Supplementary Figure S3). Collectively, these data suggest that female *Md*STING mice exhibit alleviated aging-related inflammation.

Bat STING reduces pro-inflammatory cytokines and chemokines *in vivo*

Our data suggest that *Md*STING mice exhibit improvement in the blood profiles of aging-associated secretory cytokines (SASP) during the aging process. To validate these findings *in vivo*, we selected two groups of mice—young (1.5 months) and aged (13 months)—for both the WT and *Md*STING strains for further comparison. The 13 months group was specifically chosen because it exhibited the most substantial differences in healthspan according to our previous results. We then dissected the mice and compared the expression levels of various SASP cytokines and the recruitment of pro-inflammatory white blood cells across different mouse organs

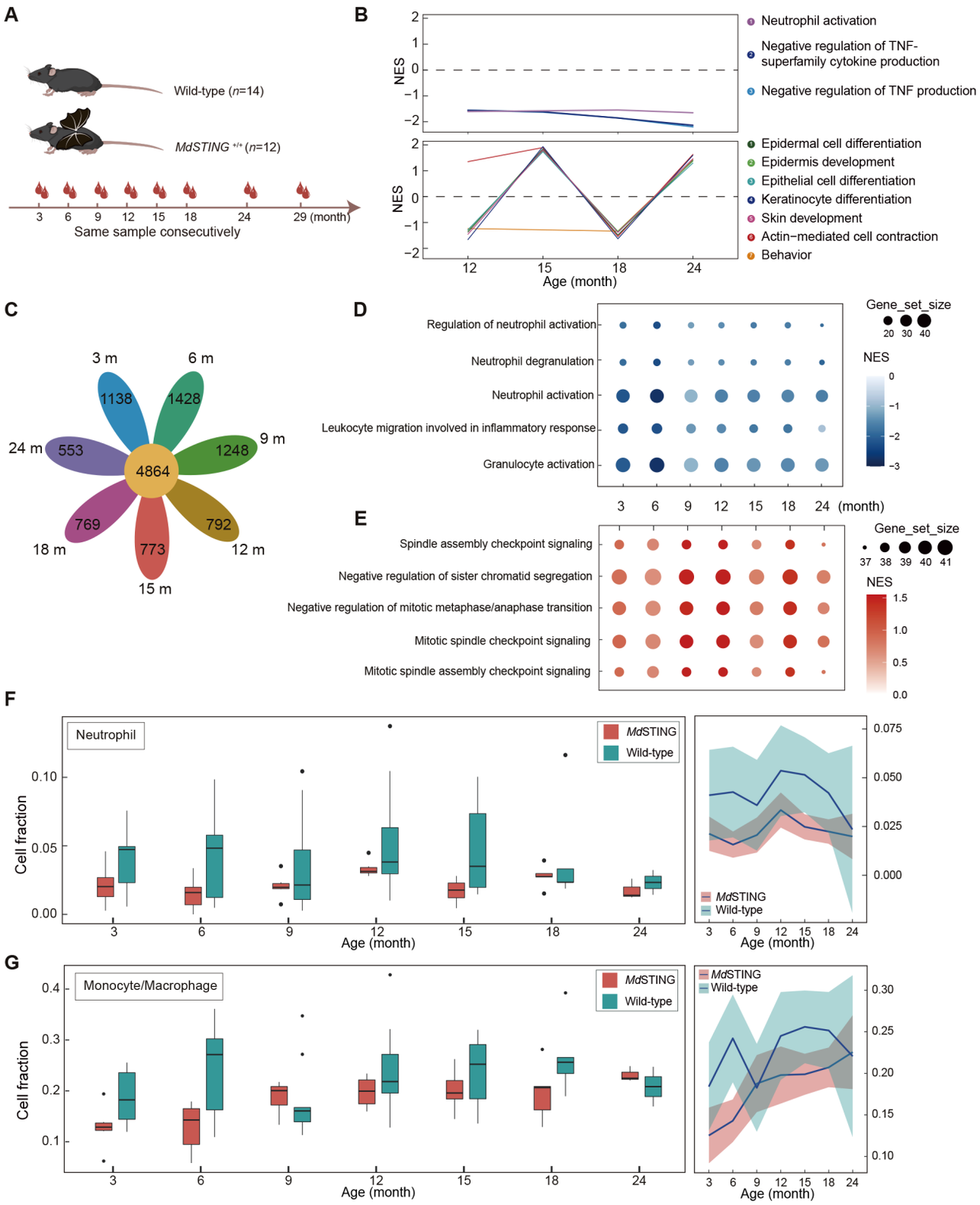

Figure 2 Longitudinal comparative blood transcriptomic analysis reveals lower aging-related inflammation in bat STING knock-in female mice

A: Schematic of longitudinal monitoring and blood testing. B: GSEA plots showing trend of significantly changed pathway in aged *Md*STING female mice during aging (upper, down-regulated; lower, up-regulated). C: Number of common or unique pathways at each time point. m: months. D: Top five pathways down-regulated at all time points in *Md*STING female mice compared to WT female mice. E: Top five pathways up-regulated at all time points in *Md*STING female mice compared to WT female mice. F, G: Neutrophil (F) and monocyte/macrophage (G) fractions in WT female mice or *Md*STING female mice, compared by ImmuCellAI, at each time point. Change trends are shown on right. Male mouse data are shown in Supplementary Figure S3.

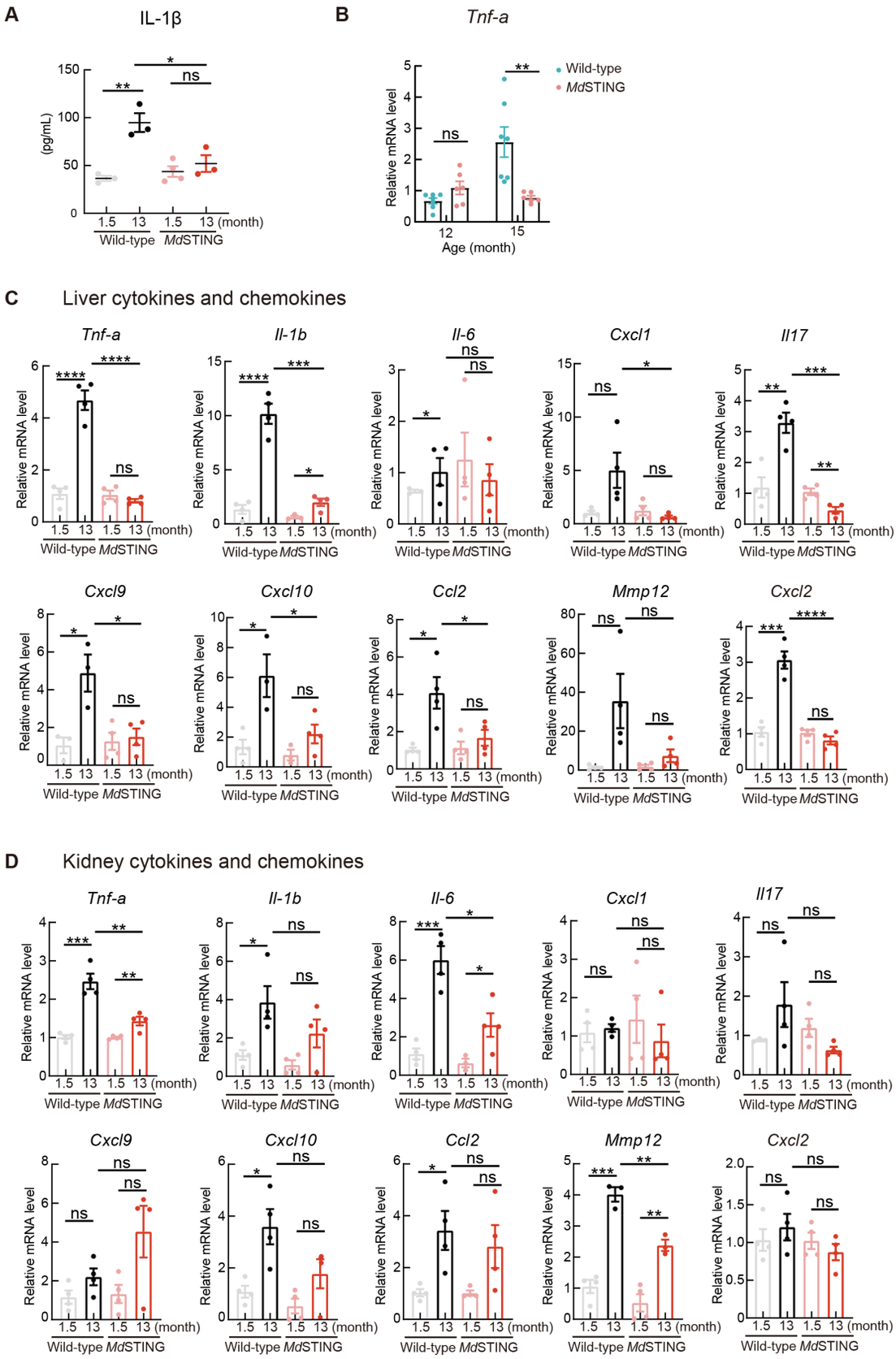

Figure 3 *Md*STING knock-in reduces pro-inflammatory response *in vivo*

A: Plasma cytokine expression was detected for IL-1β (*n*=4 WT and *Md*STING female mice). B: *Tnf-a* mRNA expression level in aged female mice. C: mRNA expression level of pro-inflammatory cytokines in mouse liver, including a panel of cytokines and chemokines (*n*=4 mice for each group). D: mRNA expression level of pro-inflammatory cytokines in mouse kidney, including a panel of cytokines and chemokines (*n*=4 mice for each group). Data are mean±SEM. *P*-values were obtained using two-tailed unpaired *t*-test, ns: Not significant; *: *P*<0.05; **: *P*<0.01; ***: *P*<0.001; ****: *P*<0.0001.

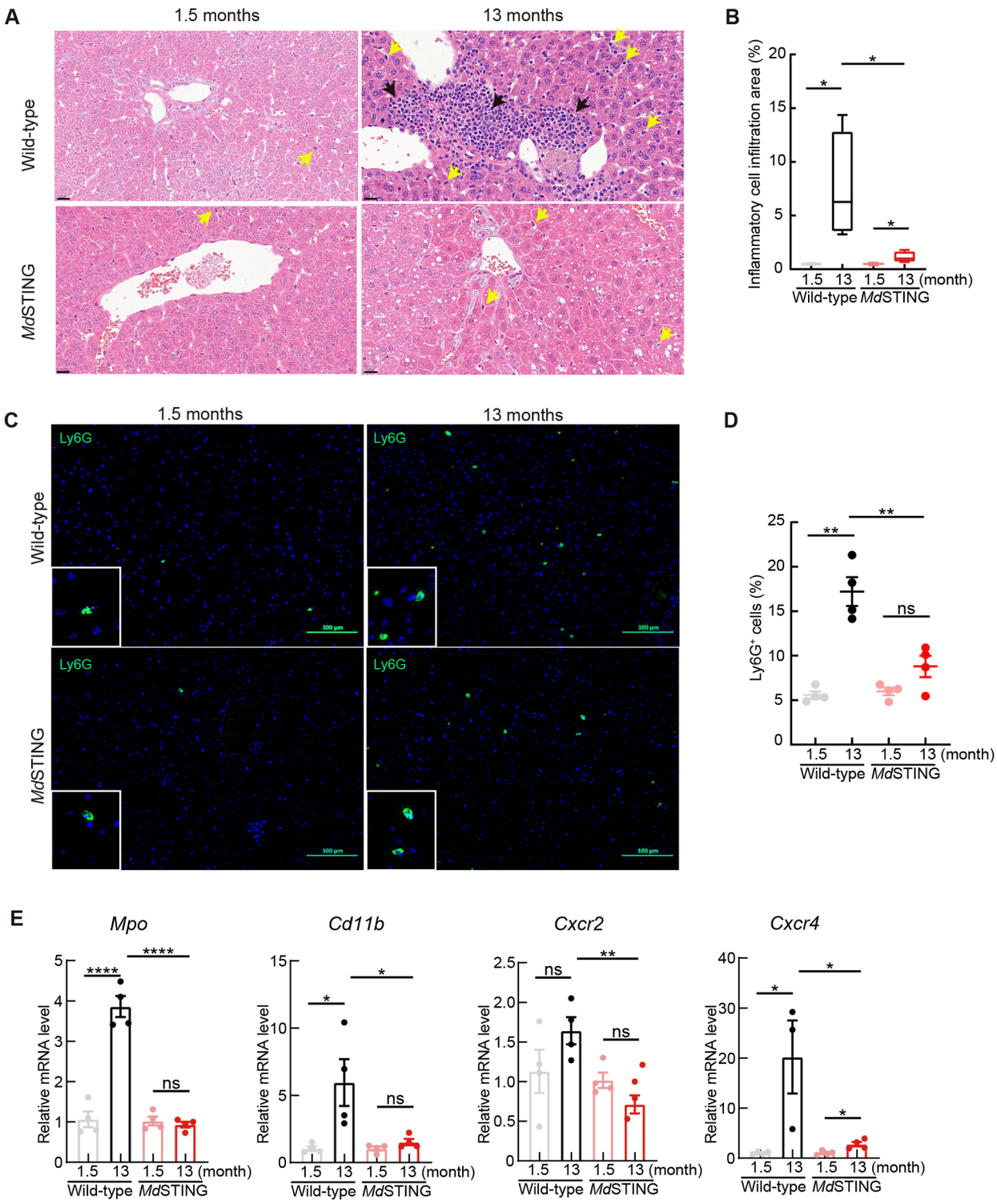

Figure 4 Bat STING reduces aging-related immunopathology

A: Immunopathological analysis of liver tissues from 1.5- and 13-month-old WT and *Md*STING female mice. H&E staining (40×) showed infiltration of inflammatory cells (black arrow) and Kupffer cells (yellow arrow) in each mouse group. Scale bars: 20 μm. B: Quantification of inflammatory cell infiltration area (n=4 for each group). C: Immunostaining of Ly6G, representing infiltration of neutrophils. D: Quantification of Ly6G-positive cells (n=4 for each group). E: mRNA expression levels of *Mpo*, *Cd11b*, *Cxcr2*, and *Cxcr4* genes, representing activation of neutrophils (n=4 for each group). Data are mean±SEM. P-values were obtained using two-tailed unpaired t-test, ns: Not significant; *: P<0.05; **: P<0.01; ***: P<0.001; ****: P<0.0001.

(Figures 3, 4; Supplementary Figure S5).

Given the marked down-regulation of the TNF pathway in *Md*STING female mice, we initially measured *Tnf-a* mRNA expression in aged female mice and serum cytokine levels across different mouse groups. Consistent with our gene expression results, both *Tnf-a* and IL-1β proteins were up-regulated during the aging process in WT female mice but not in *Md*STING female mice (Figure 3A, B). We then assessed a panel of SASP-related cytokines and chemokines in various organs, including the liver, kidney, heart, spleen, intestine,

lung, blood, and muscle. As observed in previous aging-related mouse models (Zhang et al., 2023), the liver and kidney exhibited the most pronounced phenotypic differences (Figure 3C, D; Supplementary Figure S5). Compared to young mice, aged WT mice displayed a substantial increase in SASP-related cytokines (*Tnf*, *Il1b*, and *Il17* in the liver and *Tnf*, *Il1b*, and *Il6* in the kidney) and SASP-related chemokines (*Cxcl9*, *Cxcl10*, and *Ccl2* in the liver and *Cxcl10*, *Ccl2*, and *Mmp12* in the kidney). In contrast, most of these genes either exhibited lower expression or showed no age-dependent up-regulation in *Md*STING mice. Additionally, one or more SASP-related genes (Birch & Gil, 2020) were up-regulated in aged WT mice but not in *Md*STING mice in other organs (Supplementary Figure S5A–F). These findings suggest that aging increases the expression of inflammatory genes, and STING plays a regulatory role during this process, with dampened *Md*STING resulting in reduced aging-related proinflammatory cytokines.

Bat STING reduces aging-related immunopathology in mice

Subsequently, we assessed physiological changes during the aging process, specifically immunopathological analysis of the liver, a site showing significant SASP-related cytokine differences between the WT and *Md*STING mice. The liver is susceptible to various degenerative changes, including increased inflammation and fibrosis, diminished regenerative capacity, and reduced repair ability after injury, leading to the development of related diseases during aging (Hoare et al., 2010; Zhang et al., 2023). Here, we compared 13-month-old *Md*STING and WT mice, given that mice started to show aging-related inflammation at this time point. Results showed that mild fatty lesions were observed in the aged livers (13 months) of all groups. Notably, significant foci of inflammatory cell infiltration, particularly in the Kupffer cells, were observed in the aged WT mice but not in the *Md*STING mice (Figure 4A, B). These findings suggest that *Md*STING mice exhibit reduced aging-related immunopathology compared to their WT counterparts.

Additionally, we observed a significant influx of neutrophils exclusively in aged WT mice (Figure 4C, D), aligning with our prior observation of low neutrophil activation in *Md*STING mice. To further identify indicators of liver neutrophil activation, we examined the expression of immune cell markers and cytokine receptors through qPCR. Results revealed a notably higher expression of *Cd11b* myeloid cell markers and neutrophil activation-related indicators, such as *Mpo*, *Cxcr2*, and *Cxcr4*, in aged WT mice compared to *Md*STING mice (Figure 4E). These findings, coupled with limited pathological changes, reduced immune cell recruitment, and mitigated inflammation during aging in *Md*STING mice, underscore the crucial role of bat STING in enhancing healthspan in mice.

DISCUSSION

To the best of our knowledge, this study represents the first *in vivo* exploration of the potential mechanisms underlying the exceptional longevity observed in bats. Through the utilization of a knock-in mouse model, our results showed that *Myotis* bat STING attenuated aging-related pro-inflammatory cytokines and chemokines and inhibited the recruitment of pro-inflammatory immune cells in a sex-dependent manner in mice. These findings were supported by both longitudinal comparative transcriptomic analysis and subsequent experimental validation. Building upon our previous identification of a dampened STING-interferon response (Xie et al., 2018), our results suggest that STING may play an important role in the extended lifespan of bats.

Aging in humans is a risk factor for many chronic diseases, such as cancer (Cai et al., 2022). Beyond research into human aging, there is increasing interest in exploring longevity in animals to unravel potential anti-aging mechanisms (Stenvinkel & Shiels, 2019; Tian et al., 2017; Zhao et al., 2021). Two mammals that have recently gained significant attention are naked-mole rats and bats, noted for their extended lifespans relative to similarly sized mammals (Baid et al., 2024; Gorbunova et al., 2020; Huang et al., 2019; Oka et al., 2023; Zhang et al., 2023). However, a major challenge in studying these animals is the lack of *in vivo* animal models and appropriate reagents. Recent research has shown that overexpressing high-molar-mass hyaluronic acid (HMM-HA) from the naked-mole rat significantly enhances healthspan in mice, providing valuable insights through the use of transgenic mice as a tool for studying non-model animals (Zhang et al., 2023). Similarly, while studies suggest that bats may possess unique aging-related pathways, the lack of *in vivo* data has hindered the validation of these conclusions (Huang et al., 2019; Irving et al., 2021; Li et al., 2023). In this context, our data hold important implications, showing that bat genes can mitigate aging-related inflammatory responses and potentially extend healthspan in mice. These findings highlight the utility of genetically modified mice as an *in vivo* model for investigating the anti-aging mechanisms of bats. The success of this model paves the way for further exploration of bat genes involved in DNA damage repair (e.g., P53, ATM, and SETX) (Zhao et al., 2023), which exhibit positive selection and are believed to play a role in bat longevity (Zhang et al., 2013).

Our study revealed that reduced STING functionality contributes to anti-aging effects. During the human aging process, senescence and SASP are pivotal and largely depend on the cGAS-STING pathway, which recognizes fragmented nuclear or mitochondrial DNA (Gulen et al., 2023; Hu & Shu, 2023; Victorelli et al., 2023). These aging-related danger signals contribute to a low-level pro-inflammatory state, eventually leading to chronic organ aging (Cai et al., 2022). Consequently, STING has emerged as an intriguing target for interventions aimed at addressing aging-related diseases (Huang et al., 2023; Pan et al., 2023; Zhang et al., 2022; Zhao et al., 2023). Previous research has shown that blockade of STING using the small molecule H-151 suppresses the inflammatory phenotypes of senescent human cells and tissues and attenuates aging-related inflammation in multiple peripheral organs and the brain in mice (Gulen et al., 2023). In comparison, bat STING, while naturally dampened, retains functionality (Xie et al., 2018). Our data demonstrate a similar effect, with reduced cytokine release and immune cell recruitment akin to the effects observed with H-151 or HMM-HA in mice (Gulen et al., 2023; Zhang et al., 2023). This suggests that bat STING could be a promising target for anti-aging studies, offering potential avenues for further research and therapeutic development.

Our study has several limitations, suggesting areas for improvement in future research. First, although our *in vitro* data showed attenuated aging-related inflammation in *Myotis* STING knock-in mice, we failed to observe a significant improvement in healthspan. Thus, further investigation into aging-related immunopathology in both male and female

Myotis STING knock-in mice should be performed to clarify sex-specific effects on aging (Xiao et al., 2024), especially given our findings of attenuated aging-related inflammation in *Md*STING female mice. This discrepancy may be due to the relatively small cohort size of mice compared to other aging cohorts, with the number of mice used simply insufficient for a lifespan study. Consequently, the results of this study should be considered preliminary. A more robust aging study with an appropriate number of animals is required to derive definitive aging results in future work. Second, while our data suggest a significant role for STING in bats, the precise mechanisms by which STING modulates aging-related inflammation in our model remains to be elucidated. The dampened interferon and inflammation pathways mediated by bat STING protein may play a role, but other signaling pathways may also be involved, especially considering the complexity of the aging process (Benayoun et al., 2015; López-Otín et al., 2023; Zhao et al., 2023). Validating the role of bat STING using bat models remains a critical step. Given the challenges associated with establishing bat colonies, conducting cell senescence studies using bat pluripotent stem cells or bat organoids (Déjosez et al., 2023) may be a viable alternative in future research. Third, there is potential to develop small molecules that dampen, rather than completely inhibit, the functionality of human STING (Pan et al., 2023; Zou et al., 2023), mimicking the natural dampening observed in bats. Additionally, exploring whether bat STING confers mice with resistance to viral-induced inflammation would be interesting. Such studies may shed light on the unique coexistence between bats and viruses, providing valuable insights into the complex relationship between the bat immune system and viral infections.

In summary, utilizing an *in vivo* model for studying bat anti-aging mechanisms, this study provides preliminary evidence demonstrating that *Myotis* bat STING reduces aging-related pro-inflammatory responses and pathology, possibly improving healthspan in mice. These findings underscore the potential of bat STING as a promising target for anti-aging studies and offer insights into the mechanisms that could be harnessed for improving healthspan in mammals.

DATA AVAILABILITY

The raw RNA-seq data analyzed in this study are available from the NCBI database (BioProjectID PRJNA1098971), China National Center for Bioinformation database of Genome Sequence Archive (GSA) (PRJCA025190), and Science Data Bank database (doi: 10.57760/sciencedb. j00139.00129).

SUPPLEMENTARY DATA

Supplementary data to this article can be found online.

COMPETING INTERESTS

The authors declare that they have no competing interests.

AUTHORS' CONTRIBUTIONS

P.Z. conceived the concept; X.W. and P.Z. designed the study; X.W. and J.K.J. performed the experiments; X.W. analyzed most of the data; Q.W. and J.K.J. analyzed the RNA-seq data; J.W.G. and A.L. raised the mice; J.S. collected the RNA-seq data; P.Z. and X.W. wrote and revised the manuscript. All authors read and approved the final version of the manuscript.

ACKNOWLEDGMENTS

We appreciate the help of Fan Zhang, He Zhao, and Li Li from the animal center of the Wuhan Institute of Virology.

REFERENCES

Ahn M, Anderson DE, Zhang Q, et al. 2019. Dampened NLRP3-mediated inflammation in bats and implications for a special viral reservoir host. *Nature Microbiology*, **4**(5): 789–799.

Ahn M, Chen VCW, Rozario P, et al. 2023. Bat ASC2 suppresses inflammasomes and ameliorates inflammatory diseases. *Cell*, **186**(10): 2144–2159. e22.

Austad SN. 2009. Comparative biology of aging. *The Journals of Gerontology: Series A*, **64A**(2): 199–201.

Baid K, Irving AT, Jouvenet N, et al. 2024. The translational potential of studying bat immunity. *Trends in Immunology*, **45**(3): 188–197.

Benayoun BA, Pollina EA, Brunet A. 2015. Epigenetic regulation of ageing: linking environmental inputs to genomic stability. *Nature Reviews Molecular Cell Biology*, **16**(10): 593–610.

Birch J, Gil J. 2020. Senescence and the SASP: many therapeutic avenues. *Genes & Development*, **34**(23-24): 1565–1576.

Brunet-Rossinni AK, Austad SN. 2004. Ageing studies on bats: a review. *Biogerontology*, **5**(4): 211–222.

Cai YS, Song W, Li JM, et al. 2022. The landscape of aging. *Science China Life Sciences*, **65**(12): 2354–2454.

Danecek P, Bonfield JK, Liddle J, et al. 2021. Twelve years of SAMtools and BCFtools. *GigaScience*, **10**(2): giab008.

Déjosez M, Marin A, Hughes GM, et al. 2023. Bat pluripotent stem cells reveal unusual entanglement between host and viruses. *Cell*, **186**(5): 957–974. e28.

Fu FY, Shao Q, Zhang JJ, et al. 2023. Bat STING drives IFN-beta production in anti-RNA virus innate immune response. *Frontiers in Microbiology*, **14**: 1232314.

Gorbunova V, Seluanov A, Kennedy BK. 2020. The world goes bats: living longer and tolerating viruses. *Cell Metabolism*, **32**(1): 31–43.

Gulen MF, Samson N, Keller A, et al. 2023. cGAS-STING drives ageing-related inflammation and neurodegeneration. *Nature*, **620**(7973): 374–380.

Healy K, Guillerme T, Finlay S, et al. 2014. Ecology and mode-of-life explain lifespan variation in birds and mammals. *Proceedings of the Royal Society B: Biological Sciences*, **281**(1784): 20140298.

Hoare M, Das T, Alexander G. 2010. Ageing, telomeres, senescence, and liver injury. *Journal of Hepatology*, **53**(5): 950–961.

Hu MM, Shu HB. 2023. Mitochondrial DNA-triggered innate immune response: mechanisms and diseases. *Cellular & Molecular Immunology*, **20**(12): 1403–1412.

Huang YG, Liu BY, Sinha SC, et al. 2023. Mechanism and therapeutic potential of targeting cGAS-STING signaling in neurological disorders. *Molecular Neurodegeneration*, **18**(1): 79.

Huang ZX, Whelan CV, Foley NM, et al. 2019. Longitudinal comparative transcriptomics reveals unique mechanisms underlying extended healthspan in bats. *Nature Ecology & Evolution*, **3**(7): 1110–1120.

Irving AT, Ahn M, Goh G, et al. 2021. Lessons from the host defences of bats, a unique viral reservoir. *Nature*, **589**(7842): 363–370.

Kim D, Paggi JM, Park C, et al. 2019. Graph-based genome alignment and genotyping with HISAT2 and HISAT-genotype. *Nature Biotechnology*, **37**(8): 907–915.

Li KQ, Liu GJ, Liu XY, et al. 2023. EPAS1 prevents telomeric damage-induced senescence by enhancing transcription of *TRF1, TRF2*, and *RAD50*. *Zoological Research*, **44**(3): 636–649.

López-Otín C, Blasco MA, Partridge L, et al. 2023. Hallmarks of aging: an expanding universe. *Cell*, **186**(2): 243–278.

Love MI, Huber W, Anders S. 2014. Moderated estimation of fold change and dispersion for RNA-seq data with DESeq2. *Genome Biology*, **15**(12): 550.

Ma X, Wong ASY, Tam HY, et al. 2018. *In vivo* genome editing thrives with diversified CRISPR technologies. *Zoological Research*, **39**(2): 58–71.

Miao YR, Xia MX, Luo M, et al. 2022. ImmuCellAI-mouse: a tool for comprehensive prediction of mouse immune cell abundance and immune microenvironment depiction. *Bioinformatics*, **38**(3): 785–791.

Oka K, Yamakawa M, Kawamura Y, et al. 2023. The naked mole-rat as a model for healthy aging. *Annual Review of Animal Biosciences*, **11**: 207–226.

Pan J, Fei CJ, Hu Y, et al. 2023. Current understanding of the cGAS-STING signaling pathway: Structure, regulatory mechanisms, and related diseases. *Zoological Research*, **44**(1): 183–218.

Paul BD, Snyder SH, Bohr VA. 2021. Signaling by cGAS-STING in Neurodegeneration, Neuroinflammation, and Aging. *Trends in Neurosciences*, **44**(2): 83–96.

Power ML, Foley NM, Jones G, et al. 2022. Taking flight: an ecological, evolutionary and genomic perspective on bat telomeres. *Molecular Ecology*, **31**(23): 6053–6068.

Ruiz-Aravena M, Mckee C, Gamble A, et al. 2022. Ecology, evolution and spillover of coronaviruses from bats. *Nature Reviews Microbiology*, **20**(5): 299–314.

Shumate A, Wong B, Pertea G, et al. 2022. Improved transcriptome assembly using a hybrid of long and short reads with StringTie. *PLoS Computational Biology*, **18**(6): e1009730.

Stenvinkel P, Shiels PG. 2019. Long-lived animals with negligible senescence: clues for ageing research. *Biochemical Society Transactions*, **47**(4): 1157–1164.

Subramanian A, Tamayo P, Mootha VK, et al. 2005. Gene set enrichment analysis: a knowledge-based approach for interpreting genome-wide expression profiles. *Proceedings of the National Academy of Sciences of the United States of America*, **102**(43): 15545–15550.

Teeling EC, Vernes SC, Dávalos LM, et al. 2018. Bat biology, genomes, and the Bat1K project: to generate chromosome-level genomes for all living bat species. *Annual Review of Animal Biosciences*, **6**: 23–46.

Tian X, Seluanov A, Gorbunova V. 2017. Molecular mechanisms determining lifespan in short- and long-lived species. *Trends in Endocrinology & Metabolism*, **28**(10): 722–734.

Victorelli S, Salmonowicz H, Chapman J, et al. 2023. Apoptotic stress causes mtDNA release during senescence and drives the SASP. *Nature*, **622**(7983): 627–636.

Wickham H. 2016. ggplot2: Elegant Graphics for Data Analysis. 2nd ed. Cham: Springer.

Wu TZ, Hu EQ, Xu SB, et al. 2021. clusterProfiler 4.0: A universal enrichment tool for interpreting omics data. *The Innovation*, **2**(3): 100141.

Xiao T, Lee J, Gauntner TD, et al. 2024. Hallmarks of sex bias in immuno-oncology: mechanisms and therapeutic implications. *Nature Reviews Cancer*, doi: https://doi.org/10.1038/s41568-024-00680-z.

Xie JZ, Li Y, Shen XR, et al. 2018. Dampened STING-dependent interferon activation in bats. *Cell Host & Microbe*, **23**(3): 297–301. e4.

Zhang GJ, Cowled C, Shi ZL, et al. 2013. Comparative analysis of bat genomes provides insight into the evolution of flight and immunity. *Science*, **339**(6118): 456–460.

Zhang ZH, Tian X, Lu JY, et al. 2023. Increased hyaluronan by naked mole-rat Has2 improves healthspan in mice. *Nature*, **621**(7977): 196–205.

Zhang ZL, Zhou HF, Ouyang XH, et al. 2022. Multifaceted functions of STING in human health and disease: from molecular mechanism to targeted strategy. *Signal Transduction and Targeted Therapy*, **7**(1): 394.

Zhao Y, Seluanov A, Gorbunova V. 2021. Revelations about aging and disease from unconventional vertebrate model organisms. *Annual Review of Genetics*, **55**: 135–159.

Zhao Y, Simon M, Seluanov A, et al. 2023. DNA damage and repair in age-related inflammation. *Nature Reviews Immunology*, **23**(2): 75–89.

Zhou P, Tachedjian M, Wynne JW, et al. 2016. Contraction of the type I IFN locus and unusual constitutive expression of *IFN-α* in bats. *Proceedings of the National Academy of Sciences of the United States of America*, **113**(10): 2696–2701.

Zou Y, Zhang M, Zhou JM. 2023. Recent trends in STING modulators: structures, mechanisms, and therapeutic potential. *Drug Discovery Today*, **28**(9): 103694.